Energy Conversion and Management 269 (2022) 116144

Contents lists available at ScienceDirect

Energy Conversion and Management

journal homepage: www.elsevier.com/locate/enconman

Thermodynamic limitations to direct CO_2 utilisation within a small-scale integrated biomass power cycle

Michael J. Greencorn [a], S. David Jackson [b], Justin S.J. Hargreaves [b], Souvik Datta [c,d], Manosh C. Paul [a,*]

[a] James Watt School of Engineering, University of Glasgow, UK
[b] School of Chemistry, University of Glasgow, UK
[c] Hochschule für Wirtschaft, Fachhochschule Nordwestschweiz, Olten, CH, Switzerland
[d] Center of Economic Research, ETH Zürich, CH, Switzerland

ARTICLE INFO

Keywords:
Carbon dioxide utilisation
Integrated gasification power cycle
Biomass gasification
CO_2 gasification
Thermodynamic modelling

ABSTRACT

Partially recycling CO_2-rich exhaust gases from a syngas fuelled internal combustion engine to a biomass gasifier has the capability to realise a new method for direct carbon dioxide utilisation (CDU) within a bioenergy system. Simulation of an integrated, air-blown biomass gasification power cycle was used to study thermodynamic aspects of this emerging CDU technology. Analysis of the system model at varying gasifier air ratios and exhaust recycling ratios revealed the potential for modest system improvements under limited recycling ratios. Compared to a representative base thermodynamic case with overall system efficiency of 28.14 %, employing exhaust gas recycling (EGR) enhanced gasification system efficiency to 29.24 % and reduced the specific emissions by 46.2 g-CO_2/kWh. Further investigation of the EGR-enhanced gasification system revealed the important coupling between gasification equilibrium temperature and exhaust gas temperature through the syngas lower heating value (LHV). Major limitations to the thermodynamic conditions of EGR-enhanced gasification as a CDU strategy result from the increased dilution of the syngas fuel by N_2 and CO_2 at high recycling ratios, restricting equilibrium temperatures and reducing gasification efficiency. N_2 dilution in the system reduces the efficiency by up to 2.5 % depending on the gasifier air ratio, causing a corresponding increase to specific CO_2 emissions. Thermodynamic modelling indicates pre-combustion N_2 removal from an EGR-gasification system could decrease specific CO_2 emissions by 9.73 %, emitting 118.5 g/kWh less CO_2 than the basic system.

1. Introduction

Carbon-dioxide utilisation (CDU) schemes aim to maximise the benefit derived from a source of CO_2 before the gas is released to the atmosphere or sent for long term sequestration. Often, such CDU strategies aim to create new materials derived from the chemical conversion of CO_2. Products could include bulk chemicals or building materials while some processes can even convert CO_2 into a useful fuel for further energy generation or storage. Even in situations where the CO_2 stream remains unconverted, further benefit can still be realised. Some examples of these latter, direct CDU strategies include enhanced oil recovery, heat transfer and storage, combustion dilution, and acting as a cycle working fluid [1]. Biomass energy cycles present an opportunity for potential CDU strategies to be realised within a low-carbon energy setting. Significant growth in bioenergy is anticipated as part of the shift away from fossil fuels with global annual growth rates in electricity from biomass expected to be 5–6 % over the next decade [2] while total energy derived from biomass could increase by up to 418 % by the end of the 21st century [3]. Considering this anticipated expansion of the biomass energy sector, CDU technologies are likely to have an impact on the development of this field. Furthermore, biomass energy systems using integrated gasification cycles (IGC) present mechanisms for both direct and conversion-based CDU.

Syngas produced from thermochemical gasification reactions is rich in H_2 and CO combustible species, capable for burning as a fuel. Gasifying agents used as reactants in this fuel production process can include CO_2 which is involved with the reverse Boudouard reaction and the reverse Water Gas Shift (WGS) reaction, shown in Eqs. (1) and (2) respectively. Dry reforming reactions also use CO_2 as a reactant to decompose hydrocarbons into syngas, with methane dry reforming given as an illustrative example in Eq. (3). While these reactions create

* Corresponding author.
E-mail address: Manosh.Paul@glasgow.ac.uk (M.C. Paul).

https://doi.org/10.1016/j.enconman.2022.116144
Received 12 May 2022; Received in revised form 1 August 2022; Accepted 16 August 2022
Available online 23 August 2022
0196-8904/© 2022 The Author(s). Published by Elsevier Ltd. This is an open access article under the CC BY license (http://creativecommons.org/licenses/by/4.0/).

Nomenclature

G	Gibbs free energy (kJ/mol)
T	Temperature (K)
R	Gas constant (kJ/mol-K)
C_p	Heat capacity (kJ/mol-K)
r_c	Compression ratio (-)
m	Mass quantity (kg)
n	Molar quantity (kmol)
a	Species elemental factor (-)
c_n	Correlation constants (-)
h	Specific enthalpy (kJ/mol)
h_c	Heat transfer coefficient (W/m^2-K)
ΔH_c	Enthalpy of combustion (kJ)
X_b	Burned mass fraction (-)
P	Pressure (kPa)
V	Volume (m^3)
V_c	Clearance volume (m^3)
Q	Heat energy (kJ)
W	Indicated work (kJ)
U_p	Mean piston speed (m/s)
k	Thermal conductivity (W/m-K)
K_p	Reaction equilibrium constant (-)
λ	Gasification air ratio (-)
γ	Adiabatic index (-)
∈	Crank/rod length ratio (-)
μ	Dynamic viscosity (Pa-s)
ρ	Density (kg/m^3)
θ	Engine crank angle (deg.)
η	Indicated thermal efficiency (%)

Abbreviations

A/F	Air to fuel mass ratio
imep	Indicated mean effective pressure
fmep	Friction mean effective pressure
bmep	Brake mean effective pressure
LHV	Lower heating value
IGC	Integrated gasification cycle
IGCC	Integrated gasification combined cycle
E/FGR	Exhaust (or Flue) gas recycling
EGT	Exhaust gas temperature
CGE	Cold gas efficiency
RES	Renewable energy source
CDU	Carbon dioxide utilisation
CCS	Carbon capture and storage

Subscripts

i	Syngas products
k	Gasifier inputs (feedstock and agents)
j	Element index
eng	Engine
sys	Overall system
bio	Biomass feed

CO fuel, they are endothermic thus requiring high reaction temperatures to shift their equilibrium to favour CO production [4]. Nevertheless, these reactions provide a CDU method of generating gaseous fuels from CO_2.

$$C_{(s)} + CO_2 \rightarrow 2CO; \quad \Delta\widehat{h}^0 = 172 \ \text{kJ/mol} \tag{1}$$

$$H_2 + CO_2 \leftrightarrow CO + H_2O; \quad \Delta\widehat{h}^0 = 41.2 \ \text{kJ/mol} \tag{2}$$

$$CH_4 + CO_2 \rightarrow 2H_2 + 2CO; \quad \Delta\widehat{h}^0 = 247 \ \text{kJ/mol} \tag{3}$$

Experimental studies of this CO_2 conversion phenomenon have been conducted on biomass samples gasified with CO_2 as the only gasification agent [5,6] or with CO_2 used in gasifying mixtures with H_2O [7,8] or O_2 [9,10]. Under isothermal conditions, use of CO_2 as a gasifying agent primarily influences char reduction while having negligible effects on the pyrolysis of a biomass sample [6]. Measurements during char reduction under CO_2 atmospheres show the enhancement of the reverse Boudouard reaction since CO is produced while CO_2 is consumed. Consistent with the endothermicity of the reaction, this effect is temperature dependent with CO_2 conversion increasing threefold and CO production increasing by a factor of 2.5 as the reaction temperature increases from 800 °C to 1000 °C [5]. Likewise, observations of autothermal gasification using O_2/CO_2 mixtures show the yield of CO increased by 130 % when additional CO_2 was supplied [10]. CO_2/O_2 gasification also promoted CO_2 and char conversion compared to reference cases using N_2/O_2 gasification mixtures. For example, a mixture of 40 %v/v O_2 in CO_2 resulted in 95 % char conversion while a 40 %v/v O_2 in N_2 mixture converted only 20 % of the char sample. Additionally, higher concentrations of CO_2 in the gasifying mixture allowed for complete char conversion at lower oxygen fluxes with a 25 % v/v O_2 in CO_2 mixture requiring only 35 g_{O2}/m^2s while the 40 %v/v O_2 in CO_2 mixture required nearly 80 g_{O2}/m^2s for 95 % char conversion [9].

Similar computational studies also investigated CO_2 gasification equilibrium properties [11,12,13,14]. Overall trends from these investigations highlight the capacity for enhanced char reduction, increased CO production, and potential for net-consumption of CO_2 while showing the increased endothermicity of the reaction mechanism and temperature dependency of the process. CO_2 conversion at the carbon boundary point increases with temperature, approaching 100 % as the equilibrium temperature passes 1000 °C although the minimum specific heat input for carbon conversion is reached at 850 °C. Co-gasification with oxygen and steam can improve char conversion and reduce the required energy inputs for gasification but this also reduces the CO_2 conversion of the process since the additional gasifying agents will be reacting with the feedstock [12]. There are some limitations to this effect under the integrated system conditions of Chaiwatanodom et al. [13] where gasification under a CO_2/C ratio of 1 decreased the system efficiency by 10–15 % due to the high thermal inputs required in the gasifier, although the corresponding cold gas efficiency (CGE) increased by a similar margin. These studies indicate CO_2 is an effective gasifying agent, potentially improving the performance of a biomass gasifier.

Combining a conventional gasification power cycle with a CO_2-enhanced gasifier provides a means of realising a "cycling" CDU pathway [15] where CO_2 ultimately returns to the atmosphere once the syngas is burned. While this pathway can reduce overall emissions by substituting a recycled source of CO_2 for a primary one, it cannot remove all atmospheric CO_2 emissions. When a fraction of the CO_2-rich exhaust from the power cycle is returned to the gasifier, the utilisation process is completed locally since the CO_2-derived syngas is generated and directly consumed within the same overall cycle. An additional, non-conversion CDU process is also possible if the recycled CO_2 is capable of transferring some waste heat from engine combustion to the gasifier.

Cycles incorporating this CDU strategy have been proposed for coal gasification in steam turbine cycles [16] and IGCC [17,18], and for biomass gasification in gas turbine cycles [19] where preliminary modelling highlights exhaust recycling could improve system performance. These examples of local exhaust gas recycling (EGR) enhanced

gasification are typical of large-scale, gas turbine-based, concentrated generation cycles using carbon capture and storage (CCS) technologies, typically oxy-fuel gasification/combustion.

In contrast, at the scale of distributed energy generators, internal combustion engines (ICE) are often preferred to other prime-movers due to proven operational reliability, low capital and maintenance costs, rapid ramp-up and load following characteristics, and fairly constant efficiency over a wide operating range [20,21,22]. ICE are also resilient to fuel contaminants compared to gas turbines roughly by a factor of 100 [23], an important consideration for gasification applications due to potential tar formation [24]. Furthermore, scalability of ICE make them ideal for use within a microgrid of small-scale, distributed generators [25,20] where small-scale units can be located near sources of biomass feedstocks to make best use of the resources available in an area [26].

Although some previous studies feature cycles that incorporate CO_2 recycling for gasification, their focus remains on assessing applications of CCS techniques [16,19] without directly evaluating any CDU aspects of the system. Furthermore, consideration of CO_2 gasification is generally limited to comparisons with steam recycling gasification [17], reduction of soot formation [18], or overall system efficiency [16,19]. Notwithstanding some preliminary assessments investigating the interaction of power system parameters on the gasification process [19,27], these power systems were simulated using idealised cycles instead of detailed modelling techniques. While simplified Brayton or Otto power cycle models are convenient for basic studies, as in the previous references, these models do not address combustion dynamics nor account for cycle heat losses. Considering that the recycled exhaust gas composition, temperature, and flow rate will have an influence on the gasifier thermochemical conditions, a more detailed engine model is required to account for combustion and heat transfer effects on the cycle working fluid.

1.1. Contributions of the current work

Given these limited investigations to date on direct CDU strategies used in integrated gasification cycles, an in-depth investigation is needed to fully understand how system parameters interact to influence both the overall system performance and the fundamental thermodynamics of the gasification process specifically. Complexities of such integrated systems and the coupled interdependency of component operations mean that many factors can influence the system as a whole. Additionally, the high endothermicity of the CO_2 utilisation reactions suggests gasification performance would be sensitive to any effect that changes the thermal conditions of the gasifier either through temperature or supplied allothermal heat, however this has yet to be investigated in detail within an integrated system. Particularly, an assessment of the specific benefits and limitations of implementing such a CDU strategy in a gasification power cycle is needed to inform future system designs to optimally implement EGR gasification. This is of interest in the context of small-scale distributed generation systems and internal combustion engines where gasification-based direct CDU technologies have not been explored.

In this work, we analyse the thermodynamic gasification conditions in a model representative of a small-scale, internal combustion engine-based biomass power cycle using EGR-enhanced gasification as a CDU strategy. System outputs of indicated power, efficiency, and specific emissions are studied along with resulting thermodynamic gasification parameters. This analysis focuses on the thermodynamic equilibrium conditions for gasification so that system-level effects of CO_2 recycling can be studied separate from the performance of any individual gasifier design. Specifically, the potential for carbon utilisation in the system is investigated independently of carbon capture and storage technologies to determine benefits to system efficiency and reductions to specific emissions. System parameters that influence the thermodynamics of CO_2 conversion into syngas are also highlighted. Particular focus is given to the effects of N_2 dilution within the system.

2. Proposed system

The integrated gasification cycle (IGC) is illustrated in Fig. 1. The aim of this system is to efficiently generate power from a feedstock of biomass fuel at the scale of a small, modular, distributed power generation unit. Critically, this system incorporates a recycling line from the engine exhaust to the gasifier to implement an EGR-enhanced gasification scheme for direct CDU within the system, a practice not currently used in any piston-engine based IGC. A variable fraction of the exhaust stream can be recycled in such a manner while temperatures, flow rates, and chemical composition for each line are monitored to gain detailed information on system component interactions. This allows for detailed analysis of the system response to exhaust recycling.

In the proposed system, biomass is converted to syngas in an air-blown gasifier operated at atmospheric pressure. Hot syngas is used to preheat the supplied gasification air (PRE-HEAT) to within 20 °C of the gasifier temperature. The product syngas then undergoes cyclone separation of ash and char and subsequent cooling to 40 °C (GASCOOL) to remove condensed species (DRAIN). Sufficient air for stoichiometric combustion is mixed with the syngas (CARB) and burned in an internal combustion engine to generate power (ENGINE). Exhaust gases from the engine are at high temperature and contain both CO_2 and H_2O. A portion of the flue gases are returned to the gasifier (FGR) as a source of both allothermal heat and additional gasifying agents CO_2 and H_2O, thus providing a method of using exhaust CO_2 to enhance the gasification process. Residual flue gasses are released to the atmosphere (OUT).

3. Modelling and methodology

The proposed system is modelled using Aspen Plus chemical process simulation software. Custom program scripts written in Fortran are also integrated within the simulation. In summary, the input biomass feed is interpreted in a Fortran script based on its ultimate and proximate analyses along with its calorific value and then combined with gasifying agents for the gasification sub model. After product gas cooling and separation of solid and condensed species, a Fortran script controls airflow to create a stoichiometric mixture of syngas and air for intake into a Fortran based engine model. Engine simulation is iterated until the exhaust stream properties of pressure, temperature, and composition satisfy relative convergence criteria of 0.01 %. The recycled exhaust stream is specified on a mass fraction basis and returned to the gasifier as an additional input. Overall system simulation is iterated until the syngas stream properties satisfy relative convergence criteria of 0.01 %.

3.1. Feedstock

To simulate a small generating unit, the biomass feed rate is set to 50 kg/h to give a steady input of 230 kW in terms of biomass LHV. This corresponds to an anticipated generator system output of 50 kW assuming approximate conversion efficiencies of 80 % for the gasifier and 30 % for the engine. A model representative of industrial wood residues (sawdust) is approximated in terms of a proximate and ultimate analysis [28], as shown in Table 1.

3.2. Gasification model

Biomass gasification is simulated using a non-stoichiometric, thermodynamic equilibrium method [13]. Since the current analysis aims to investigate the thermodynamic conditions underlying the gasification process, this approach is particularly useful. The fundamental basis of this model is that under equilibrium conditions, the Gibbs free energy of the syngas mixture is minimized. By prescribing both the expected syngas chemical products and the reaction conditions, the model solves a system of equations describing the minimisation of the syngas Gibbs free energy (equation (4)) constrained by an elemental mass balance (equation (5)). In this study, syngas species of H_2, CO, CH_4, CO_2, H_2O,

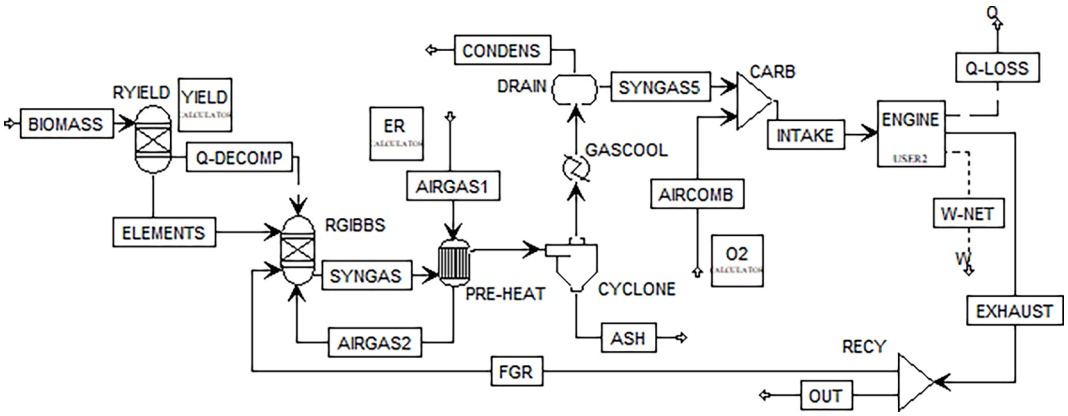

Fig. 1. Schematic of simulated biomass IGC with recycled exhaust.

Table 1
Proximate and ultimate analyses of wood sawdust pellets [28].

Proximate Analysis (wt%)				
Moisture	Volatile Matter	Fixed Carbon	Ash	LHV (MJ/kg)
9.5% (ar)	80.63 % (dry)	17.27 % (dry)	2.10 % (dry)	18.43 (dry)
Ultimate Analysis (wt%)				
C	H	N	O	
48.91 % (daf)	5.80 % (daf)	0.18 % (daf)	45.11 % (daf)	

* (ar. as received, daf. dry, ash free).

N_2, and solid carbon char residues are considered as the possible outputs of the gasifier. Gasification temperature is also solved by considering an enthalpy balance across the reactor control volume (equations (6) and (7)). For the system presented here, the gasifier is assumed to be adiabatic and is directly heated by using air as the primary gasification agent. Additional allothermal heat is introduced only through the recycled exhaust mass flow, thus indirect heating is neglected. Gasification is specified to occur under atmospheric pressure while the reaction temperature is a dependent parameter, calculated as described above.

$$G_{total} = \sum_i n_i \Delta G^0_{f,i} + \sum_i n_i \hat{R} T ln\left(\frac{n_i}{\sum n_i}\frac{P}{P^0}\right) \quad (4)$$

$$n_j = \sum_i a_{ij} n_i = \sum_k a_{kj} n_k \quad (5)$$

$$\sum_k n_k \cdot \hat{h}_k + Q_{indirect} = \sum_i n_i \cdot \hat{h}_i \quad (6)$$

$$\hat{h}_i = \hat{h}^0_{f,i} + \int_{T_0}^{T} C_{p,i} dT \quad (7)$$

Gasifying agent supply is quantified in terms of the gasification air equivalence ratio, λ, for air and a CO_2 recycling ratio for engine exhaust. The former compares the air supplied to the amount required for complete combustion of the biomass feedstock while the latter is a molar ratio of the recycled CO_2 to carbon supplied in the feedstock.

$$CO_2 \ \ recycling \ \ ratio = \frac{CO_2 \ \ recycled \ \ (mol/s)}{C \ \ in \ \ biomass \ \ (mol/kg_b) \times \dot{m}_b (kg/s)} \quad (8)$$

3.2.1. Gasification model validation

Gasification is a complex process, sensitive to many operational and design parameters. The focus of the current work is on the system-level effects of CO_2 recycling on the thermodynamic conditions of gasification rather than a detailed design analysis for specific gasifiers. Consequently, only a 0-dimensional equilibrium model is capable of such an analysis since empirical, kinetic, or CFD models will be dependent on the exact design and geometry of a chosen reactor [4]. Indeed, equilibrium models are often the preferred method for assessing complex systems with integrated gasifcation cycles [29,30,13,19].

Previous work [27] has demonstrated this model matches predictions from comparable thermodynamic simulations in the literature. Fig. 2 further highlights the agreement between this model and a range of published thermodynamic equilibrium models for gasification.

Thermodynamic studies of Ravikiran et al. [11] and Renganathan et al. [12] used this modelling approach to study gasification conditions across a range of simulated feedstock H/C/O compositions. Relevant parameters of these studies were the volumetric composition of H_2, CO, CO_2, and CH_4 in the dry syngas, the carbon residual (1-X_C), and the equilibrium temperature. The model developed for the present study shows strong agreement with these simulations for oxygen and steam gasification of a feedstock of $CH_{0.9}O_{0.45}$ under adiabatic conditions (Fig. 2 a & b). Similarly, the current model matches the results for pure CO_2 gasification of a simulated feedstock with relative mass composition of 46 % C, 6 % H, and 48 % O under isothermal conditions at 850 °C. This study also reported the relative conversion of CO_2 (X_{CO2}) alongside the volumetric composition of the dry syngas (Fig. 2 c).

Non-stoichiometric thermodynamic gasification models have also been incorporated into integrated cycle simulations, as in the work of Prabowo et al. [19]. Here, a simulated feedstock representative of coconut shells (49.3 % C, 5.5 % H, 45.0 % O) drives an integrated power cycle where it is gasified with O_2 and recycled CO_2 to generate syngas. Again, the current model generates similar gasification results to those reported in the referenced study for a gasifier temperature of 850 °C (Fig. 2 d). This configuration assumes an adiabatic gasification model while controlling the supply of O_2 gasifying agent to maintain the desired reaction equilibrium temperature.

Although the focus of the current work is to analyse the thermodynamic conditions of gasification within the integrated system, this approach can also approximate specific gasification tests. Additional validation data from Table 2 confirms the model can replicate experimental, downdraft gasification conditions [28]. The feedstock for this study is a wood sawdust with the same properties described in Table 1 while the gasifier was a pilot scale unit designed for a nominal 200 kW thermal input with a 0.3 m diameter throat. Under steady state conditions, the temperature profile ranged from 334 °C above the air inlet to peak temperatures of 1100 °C in the throat's combustion zone before dropping across the reduction zone to reach an outlet temperature of 350 °C. While the equilibrium model is zero-dimensional and thus will not reproduce a temperature gradient, the calculated equilibrium temperature of 625 °C is nevertheless representative of the reduction zone temperature partway between the combustion zone and the outlet.

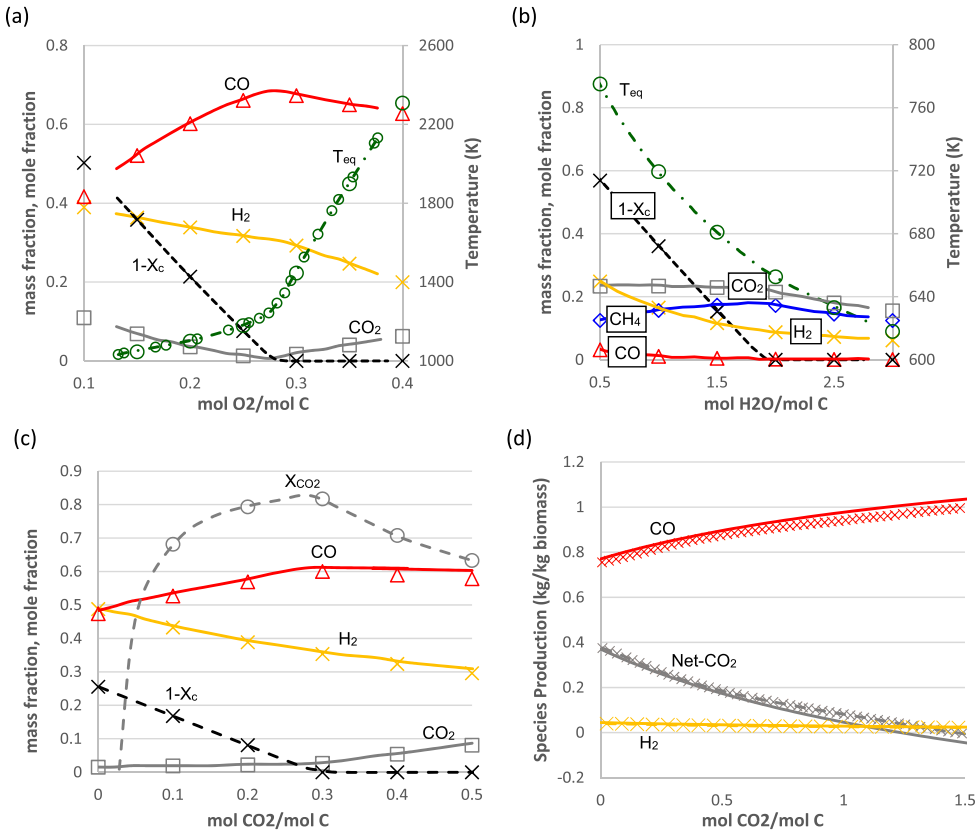

Fig. 2. Comparisons of the developed gasifier model with numerical results showing key syngas species, carbon conversion, CO_2 conversion, and equilibrium temperature as appropriate from a) oxygen & b) steam adiabatic gasification of Ravikiran et al. [11], c) isothermal CO_2 gasification of Renganathan et al. [12], and d) adiabatic gasification with recycled CO_2 of Prabowo et al. [19]. Lines represent published results while markers signify current simulation outputs.

Table 2
Comparison of syngas composition as predicted by the developed Aspen equilibrium model and measured experimentally by Simone et al [28] for wood sawdust pellets in air at an air ratio λ = 0.3.

Experiment		Gas Composition (%vol)				
		H_2	CO	CO_2	CH_4	N_2
Current model		19.73	19.97	12.66	2.44	39.91
Simone et al. [28]	Test 1	17.5	21.3	13.3	3.1	44.2
	Test 2	17.6	21.6	12.0	2.3	46.0
	Test 3	16.3	21.3	12.4	2.3	47.2

Comparing the syngas compositions illustrates common limitations of a purely thermodynamic assessment of gasification conditions. Slight overpredictions in the H_2 content and under predictions of the CO content are evident here. While simulated methane production appears to closely match the experimental results in this instance, methane is generally not a thermodynamically favourable product under typical gasification conditions and equilibrium models tend to under predict methane content is syngas. Similarly, higher carbon compounds like tars are not thermodynamically favoured and will not be accurately modelled under equilibrium conditions. Tar formation and subsequent cracking is understood to be a kinetic phenomenon of gasification [24] and is highly variable based on operating conditions, reactor geometry, and gasifier design. Even though syngas tar content is an important, practical consideration of integrated gasification power cycles, evaluation of tars is best suited to detailed design studies of specific gasification reactors and is not within the scope of this thermodynamic assessment.

3.3. Engine model

Performance of the internal combustion engine is modelled with a series of differential equations (9)-(11) that align with established methods of time-dependent engine simulation [31,32]. Solutions to the system of equations are calculated in a Fortran subroutine using a fourth order Runge-Kutta method and integrated over the engine cycle to determine the indicated net work, heat transfer, and exhaust properties.

$$\frac{dP}{d\theta} = \frac{\gamma - 1}{V}\cdot\left(\Delta H_c \cdot \frac{dX_b}{d\theta} - \frac{dQ_L}{d\theta}\right) - \frac{\gamma \cdot P}{V}\cdot\frac{dV}{d\theta} + \left[\frac{\gamma - 1}{V}\left(\frac{\gamma_0 T_0 \widehat{R}}{\gamma_0 - 1}\right)\cdot\frac{dm}{d\theta}\right] \tag{9}$$

$$\frac{dV}{d\theta} = \frac{V_c\cdot(r_c - 1)}{2} sin(\theta)\cdot(1 + \epsilon cos(\theta)) \tag{10}$$

$$\frac{dW}{d\theta} = P\cdot\frac{dV}{d\theta} \tag{11}$$

Combustion heat release is modelled using a Weibe function (eq (12)) to calculate the mass burn fraction. The standard Weibe function for petrol combustion uses parameters $c_1 = 5$ and $c_2 = 3$ [31], however the combustion dynamics of syngas are not like this case. Mass burn parameters tuned specifically for syngas combustion are employed to capture the characteristics of a syngas fuelled engine. Values of $c_1 = 2.23$ and $c_2 = 1.71$ are shown to give good results for syngas fuelled engines across many configurations and operating points [33] and are used for this present study. Fig. 3 compares the combustion profile used in this simulation to experimental measurements of syngas combustion in an ICE while highlighting the difference in combustion dynamics between syngas and the traditional Weibe function used for petrol.

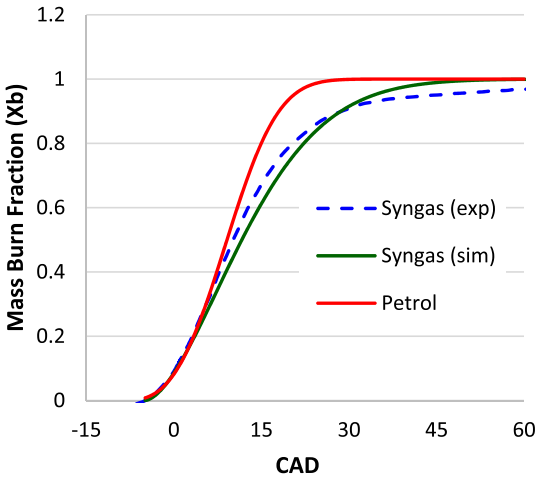

Fig. 3. In-cylinder combustion curves for petrol, simulated syngas, and experimental syngas combustion from [33].

$$X_b(\theta) = 1 - exp^{-c_1\left(\frac{\theta-\theta_s}{\theta_d}\right)^{c_2}} \quad (12)$$

Instantaneous cylinder heat loss is calculated using a fundamental Nusselt-Reynolds number relationship established by Annand [34] to determine the heat transfer coefficient, h_c. Correlation parameters of $c_3 = 0.76$ and $c_4 = 0.71$ are used to simulate heat transfer conditions for models similar to a 6-cylinder, 5.9 L engine run on syngas with a constant cylinder wall temperature [33].

$$h_c = c_3 k B^{c_4-1}\left(\frac{\rho \overline{U}_p}{\mu}\right)^{c_4} \quad (13)$$

Exhaust blowdown and residual mass fractions are also calculated at the end of each iterated engine cycle [31].

For a small, distributed generator, the dimensions of a typical four stroke, 6-cylinder, 5.9 L, spark ignited (SI) engine is chosen for the model. When run on natural gas, the engine has a rated brake output of 50 kW. Specifications of the engine simulated are provided in Table 3. The engine air/fuel ratio was set for complete stoichiometric combustion of the supplied syngas. While a detailed engine model is central to the work at hand, the present analysis focuses on the system-level integration of CO_2 gasification. As such, variations of engine parameters, including combustion equivalence ratio, were not considered.

3.3.1. Engine model validation

Validation cases using syngas (19 % H_2, 18 % CO, 1.8 % CH_4, 12 % CO_2, 49.2 % N_2) at an A/F ratio of 1.27 and inlet pressure of 78.9 kPa were compared to experimental data available in the literature [35]. Indicated power calculated by the simulation was converted to brake power by approximating the fmep based on the engine speed [31] and determining the bmep from the imep calculated by the in-cylinder simulation. At power settings ranging from 5 kW to 27 kW, both the simulated brake power and in-cylinder pressure traces agree closely with the experimentally measured data, as demonstrated in Fig. 4.

Similar agreement is shown in the engine's overall energy distribution for a similar case with 123.5 kW of thermal input [35]. Some discrepancy in exhaust sensible energy is noted, however experimental determination of this parameter was based on measured exhaust manifold temperatures. Any heat losses from the exhaust manifold would cause the experimental exhaust sensible load to appear lower than the modelling case.

Table 3
Simulated engine specifications.

Cylinders	6	–
Bore	102	mm
Stroke	120	mm
Connecting rod	192	mm
Compression ratio	10.5	–
Engine cycle	4	stroke

3.4. Exhaust gas recycling

The exhaust gas stream leaving the engine model is split with one branch returning to the gasifier as stream FGR in Fig. 1. Parameters of the FGR stream are identical to the exhaust stream leaving the engine in terms of component mole fractions, pressure, and temperature while the total stream mass flow is a specified fraction of the exhaust stream. This stream becomes an additional gasifying agent input to the gasification sub model. To study the effects of FGR enhanced gasification, successive iterations of the system model vary the mass fraction of exhaust gases recycled to the gasifier from this point. The range of CO_2 recycling ratios is set to encompass a baseline where no exhaust is recycled to the gasifier and extend to recycling ratios slightly beyond the 1.6 molCO_2/molC ratio reported in the experiments of Prabowo et al. [10]. Remaining flue gases are released from the system through a flue stack, stream OUT in Fig. 1.

4. Results and discussion

A preliminary case of the simulated IGC at a gasification air ratio of $\lambda = 0.3$ without any exhaust recycling provides a baseline for the system performance. Syngas generated under these conditions is typical of the products of air gasification. The gaseous products were 22.24 % H_2, 28.89 % CO, 7.42 % CO_2, and 41.45 % N_2 by volume with negligible CH_4, having a LHV of 6.19 MJ/Nm^3 (6.08 MJ/kg) while the equilibrium gasification temperature was 972 °C. This results in a gasifier cold gas efficiency (CGE) of 82.13 %.

Engine performance under these conditions generated 65.18 kW of indicated power with a cylinder cooling load of 61.93 kW, giving an engine thermal efficiency, η_{eng}, of 34.80 % and an exhaust temperature of 604 °C. Compared to the total thermal energy input from the biomass feeding rate, the overall IGC system has an indicated efficiency, η_{sys}, of 28.14 %.

$$CGE = \frac{\dot{n}_{syn}\cdot\overline{LHV}_{syn}}{\dot{m}_{bio}\cdot LHV_{bio}} \times 100\% \quad (14)$$

$$\eta_{eng} = \frac{\dot{W}_{net}}{\dot{n}_{syn}\cdot\overline{LHV}_{syn}} \times 100\% \quad (15)$$

$$\eta_{sys} = \frac{\dot{W}_{net}}{\dot{m}_{bio}\cdot LHV_{bio}} \times 100\% \quad (16)$$

4.1. Effect of exhaust recycling

To examine the potential use of exhaust gases in a CO_2 utilisation scheme to enhance gasification performance, the model is adapted to recycle a portion of the engine exhaust to the gasifier. Recycled exhaust is quantified by the amount of CO_2 returned to the gasifier through the molar recycling ratio (equation (8)). While this ratio is defined in terms of CO_2 recycling, the exhaust gases returned to the gasifier will also contain some water vapour as a co-product of the engine's combustion reaction.

4.1.1. Constant air ratio cases

An integrated exhaust recycling gasifier represents a complex gasification system since flowrates of gasifying agents, supplied allothermal heat, and equilibrium temperatures are all coupled with the contents of the produced syngas. Fig. 5 presents data for the syngas generated under various amounts of exhaust recycling while the gasification air flow, and

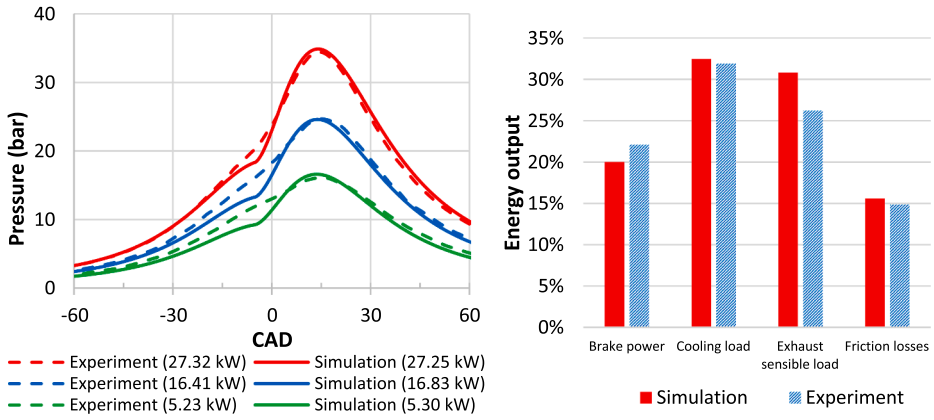

Fig. 4. Validation of the simulated engine model and empirical engine performance for (left) cylinder pressure traces and shown brake power outputs at different power settings and (right) distribution of energy output from experimental data and simulated model.

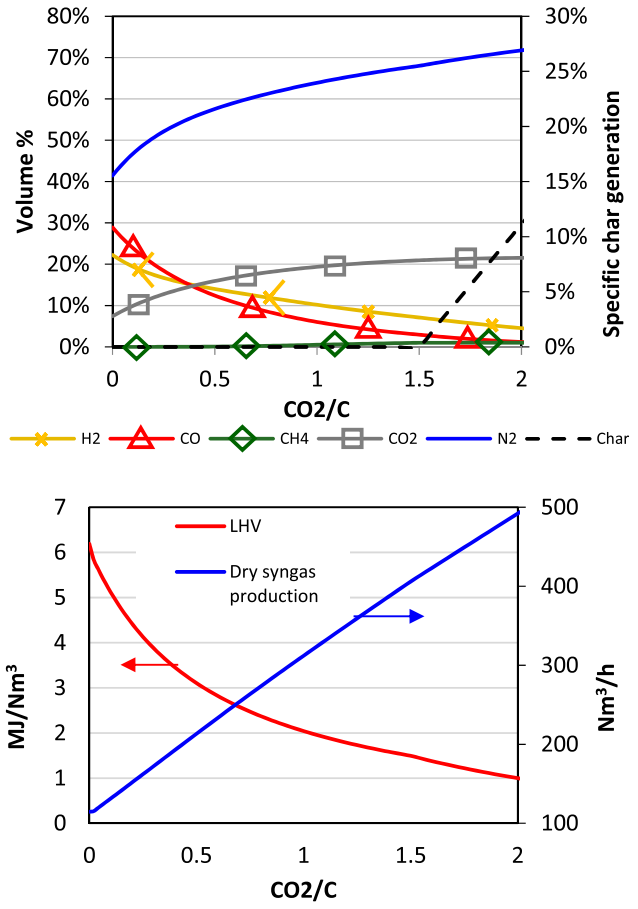

Fig. 5. Dry syngas composition and unconverted char residual (top) and dry syngas LHV and production rate (bottom) for air gasification at $\lambda = 0.300$ enhanced with recycled engine exhaust gases.

thus air ratio, is held constant at $\lambda = 0.3$. As more exhaust gases are returned to the gasifier the total volume of syngas increases accordingly. Despite a modest increase in the total H_2 production from 0.348 mol/s to a maximum of 0.396 mol/s at a recycling ratio of 0.923 molCO_2/molC, the higher total volume of produced gas decreases the fraction of H_2 in the syngas as the recycling ratio goes up. Furthermore, a slight decrease in the total production of CO from 0.399 mol/s to 0.248 mol/s over the same range of recycling ratios contributes to an increase in the H_2/CO ratio. Both H_2 and CO production drop off dramatically as the recycling ratio passes 1.0 molCO_2/molC. A minor increase to the CH_4 content is also evident as the recycling ratio rises, reaching 0.063 mol/s at the maximum recycling ratio. Additionally, there are significant increases to the N_2 and CO_2 content as exhaust gases are recycled. This dilution of the syngas with N_2 and CO_2 has the consequence of decreasing the syngas LHV with increased exhaust recycling. Sources of these diluents within the gasifier system are the N_2 introduced with the gasification air stream and the N_2 contained in the recycled exhaust gas since air is also used as the oxidizer in the combustion engine. The CO_2 diluent is generated from both the gasification and combustion processes.

Under this system configuration, gasifier temperatures decrease with increasing exhaust recycling (Fig. 6), creating thermodynamic conditions less favourable to endothermic reactions. As the recycling ratio exceeds 1.5 mol CO_2/mol C, the gasifier equilibrium condition can no longer convert all the carbon contained in the biomass feed into gases and char residues are produced. This behaviour is also reflected in the observed cold gas efficiency (CGE) where initial efficiency losses due to declining syngas LHV are moderate but significantly drop off beyond the carbon boundary point noted above. In principle, this gasifier performance agrees with previous thermodynamic studies of CO_2 gasification [12] where lower gasification temperatures, incomplete carbon conversion, and poor CGE were observed with increased supply of a CO_2 gasifying agent. Increases in the H_2:CO ratio and syngas dilution were also associated with lower gasification temperatures.

Despite the decreasing quality of the syngas, engine performance (Fig. 6) shows a marginal improvement in indicated power of 170 W for low levels of exhaust recycling. Since gasifier performance decreased under these same conditions, this phenomenon is attributable to the excess N_2 and CO_2 acting as a combustion diluent within the engine, lowering the average cylinder temperatures. With lower combustion temperatures, less charge energy is lost to the engine coolant so a higher proportion of the available energy can be transferred to useful work. Furthermore, higher CO_2 concentrations in the cylinder working fluid have previously shown limited improvement to engine performance due to changes in thermal properties [36]. This has diminishing returns, however, since the specific LHV of the fuel is decreasing overall as the recycling ratio increases.

Moreover, the lower combustion temperatures from the lower LHV fuel produce lower exhaust temperatures. In this coupled system, these exhaust gas temperatures (EGTs) have an effect on the gasification process since the recycled exhaust gases also act as a source of allothermal heat in the gasifier. The conditions of this case produced EGTs that were always cooler than the corresponding gasification temperature, limiting this benefit to the gasifier. High EGR can also lower the gasification temperature by encouraging endothermic reactions since higher concentrations of CO_2 and H_2O will tend to push the equilibrium point of the reverse Boudouard and primary water-gas char reduction

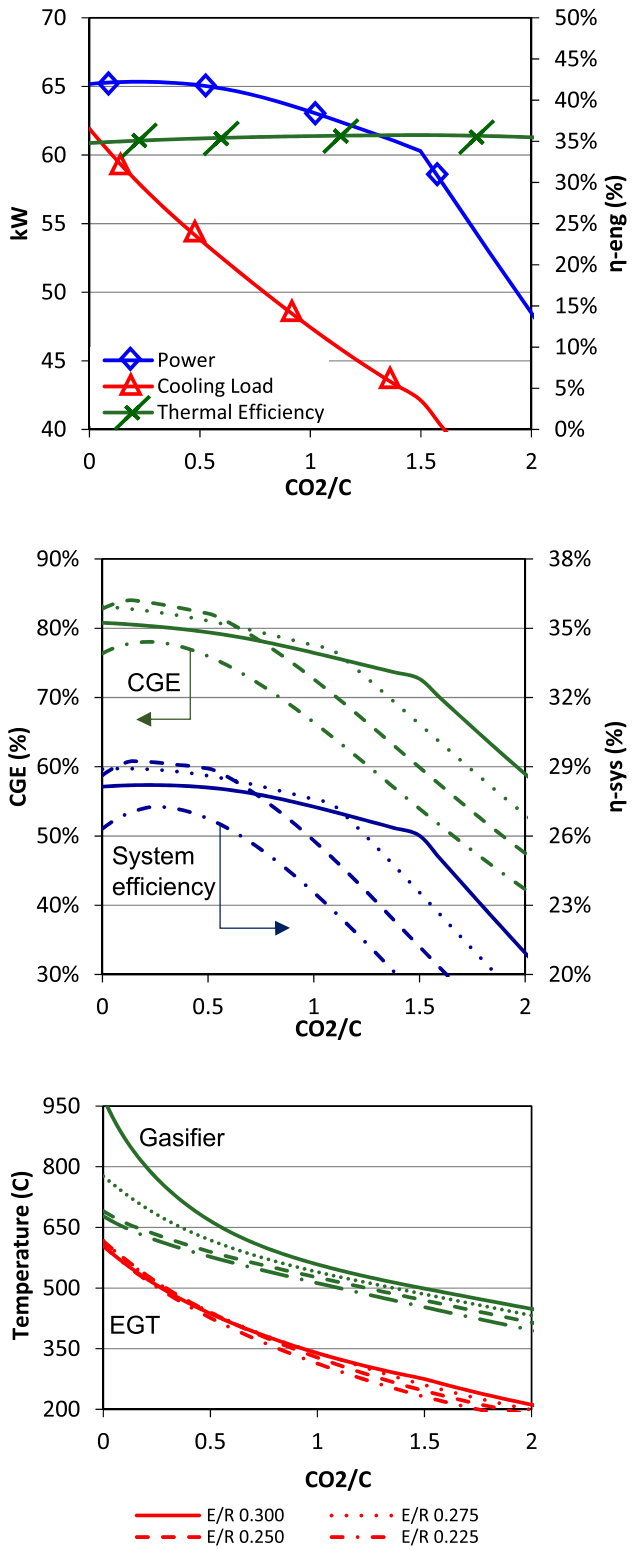

Fig. 6. System performance parameters under varying degrees of exhaust recycling showing (top) engine performance, (middle) CGE in green and total system efficiency in blue for different E/R, and (bottom) EGT in red and gasification temperature in green at different E/R.

reactions. Lower equilibrium temperatures however will tend to favour the exothermic water-gas shift reaction, hence the increasing H_2:CO ratio. In total, EGR gasification for this case showed minimal benefit, increasing the system efficiency to only 28.21 % at a recycling ratio of 0.219 molCO_2/molC.

4.1.2. Varying gasifier air ratio

Although the previous case demonstrated only minor system benefits for recycling engine exhaust, CO_2 gasification is known to enhance char conversion [9], potentially improving gasification conditions under lower air ratios. The initial air ratio of $\lambda = 0.300$ was capable of generating a good quality syngas and completely converting the biomass carbon content to syngas. However, higher air ratios would actually decrease the quality of syngas since additional oxygen would promote more combustion, generating higher temperatures and more CO_2 and H_2O rather than fuel species. On the other hand, an air equivalence ratio too low would produce temperatures too cold for effective gasification and cause low carbon conversion.

To further investigate the interaction of exhaust gas enhanced gasification and air ratio, four different air ratio cases are studied while varying amounts of exhaust gases are recycled to the gasifier. Equivalence ratios were chosen to cover a range of simulations where carbon conversion varied depending on CO_2 recycling. The baseline $\lambda = 0.300$ showed complete carbon conversion without the need for any CO_2 recycling while the extreme rich condition of $\lambda = 0.225$ was not capable of complete carbon conversion at any recycling ratio. Fig. 7 illustrates the syngas composition for these cases. Trends in gaseous species concentration remain similar across all the studied air ratios, with N_2 and CO_2 dilution remaining as a significant feature of increased recycling. However, observable differences in char production highlight a notable feature of EGR enhanced gasification. While $\lambda = 0.275$ appears to be sufficient to fully convert the biomass carbon without EGR, a lower $\lambda = 0.250$ can only achieve full conversion with some exhaust recycling. Finally, no amount of exhaust recycling is capable of complete carbon conversion for the lowest $\lambda = 0.225$ case in this system configuration.

Gasifier CGEs for these cases (Fig. 6) highlight the benefit of full carbon conversion at the lowest possible air ratio, as the peak CGE of 84.06 % and system efficiency of 29.24 % correspond to the $\lambda = 0.250$ case with a recycling ratio of 0.136 mol CO_2/mole C. The $\lambda = 0.275$ case showed trends in efficiencies similar to the original case of $\lambda = 0.300$ with initial efficiencies slightly higher, indicating the original air ratio was higher than necessary. Finally, the $\lambda = 0.225$ case demonstrates some of the limitations of air ratio reductions as its efficiencies were lower than the base case regardless of amount of exhaust recycling.

One reason for the incomplete carbon conversion at low air ratios is the lower gasification temperatures. Supplying air is what allows for partial oxidation of some of the feedstock, providing the needed energy to drive the gasification reactions. Although the $\lambda = 0.250$ case was successfully able to supplement some autothermal heat with recycled exhaust heat, the exhaust temperatures in the $\lambda = 0.225$ case were not hot enough to compensate for the low air ratio, despite the recycled exhaust heat.

4.1.3. Constant temperature gasification

The previous simulations showed that equilibrium temperatures were influenced by exhaust recycling when gasification air supply remained fixed. Since the air ratio in the gasifier has the strongest influence over the gasification temperature, control of the air flow can effectively set the gasification temperature. By manipulating the airflow into the adiabatic gasifier model, three additional simulations for constant gasifier temperatures of 650 °C, 700 °C, and 750 °C were analysed for system performance.

For these cases, equilibrium temperatures over 700 °C caused full char conversion without any exhaust recycling while only the 650 °C gasification case required EGR of at least 0.163 mol CO_2/mol C for complete carbon conversion. This latter case also had the highest efficiencies of 83.94 % for CGE and 29.23 % for the overall system efficiency occurring at the carbon boundary point (Fig. 8). Recycled gas temperatures significantly limit EGR benefits in these cases since EGTs become increasingly colder than the target gasifier temperature. This

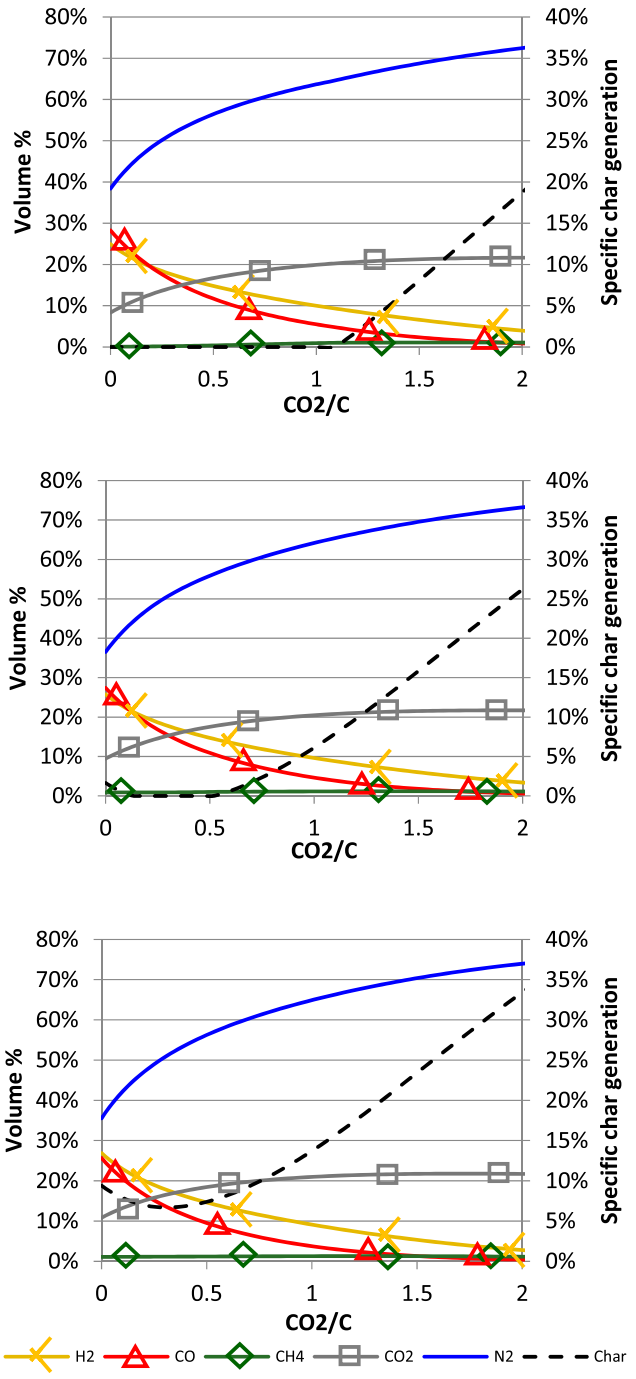

Fig. 7. Dry syngas composition and unconverted char residual for air gasification enhanced with recycled engine exhaust gases at λ = 0.275 (top), λ = 0.250 (centre), and λ = 0.225 (bottom).

has the effect of requiring additional sensible heat to bring these reactants up to temperature, forcing ever higher air ratios in the gasifier to maintain the desired equilibrium temperature (Fig. 8 c).

4.2. Effect of excess diluents

From the previous analyses, it is evident that temperature differences between the recycled exhaust and the gasifier cause limitations to the benefits of EGR gasification. It was also shown that the dilution of the syngas with N_2 contributes to the low EGT that exacerbates this issue. In order to quantitatively examine this aspect of the integrated gasification

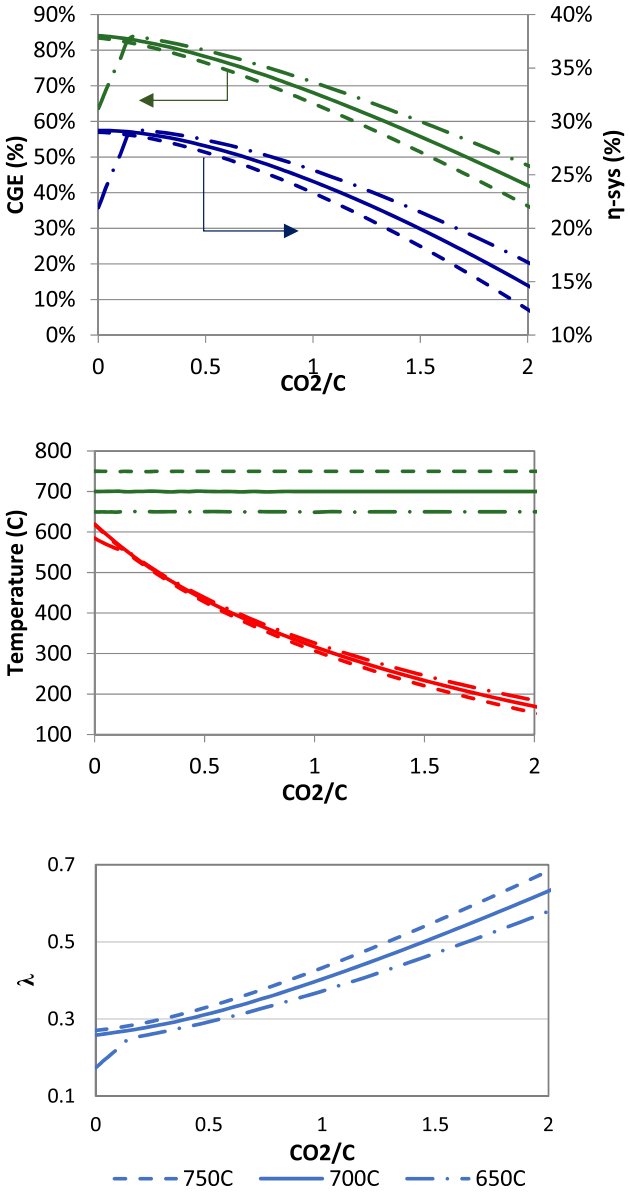

Fig. 8. CGE in green and system efficiency in blue (top), EGT in red and gasifier temperature in green (centre), and required air ratio (bottom) for constant gasifier temperatures.

system, two separate modelling cases are considered where N_2 is artificially removed from the modelled system; one where N_2 is eliminated from the syngas stream and another where it is instead removed from the recycled exhaust stream. Both cases remove the diluent downstream from one of the two sources where it originates: in the gasifier air or the combustion air.

Under constant air ratio configurations, Fig. 9 indicates removal of N_2 from the syngas stream prior to combustion in the engine has the strongest impact on overall system efficiency. Less diluent during combustion results in an initial EGT roughly 100 °C higher than the baseline case, a trend which continues to improve across all recycling ratios. This beneficial influence on the total system efficiency demonstrates the improved allothermal heating supplied by the recycled exhaust gases at higher temperatures. For the λ = 0.250 case the EGT actually exceeds the gasifier temperature for low recycling ratios (Fig. 10) and increases the overall system efficiency to a maximum of 31.02 % at a recycling ratio of 0.220 mol CO_2/mol C.

Both scenarios of N_2 removal demonstrate the effect of diluent build

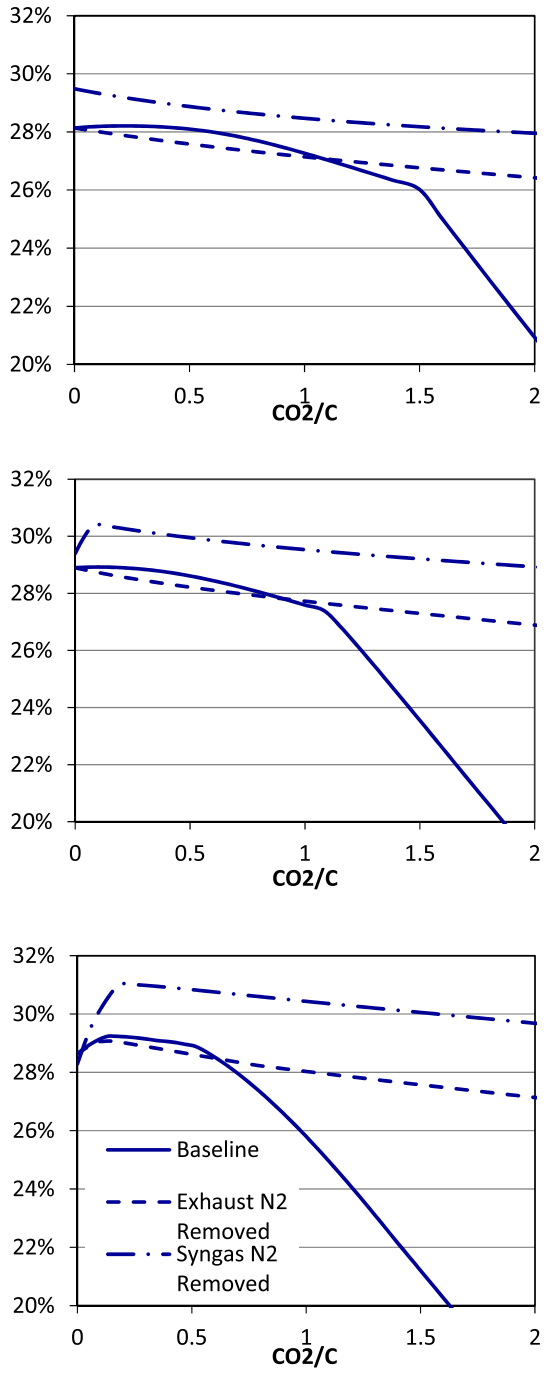

Fig. 9. System efficiencies at λ = 0.300 (top), λ = 0.275 (centre), and λ = 0.250 (bottom) for different diluent removal strategies.

up within the exhaust recycling system. The rates of change in system efficiency for both removal scenarios are approximately identical after any local efficiency peak, showing the effect of CO_2 build up when it is isolated from the long-term build-up of N_2 within the system. Similarly, the offset between the efficiency curves indicates the impact of pre-combustion versus post-combustion diluent removal. For the λ = 0.300 air equivalence ratio, this difference was ~ 1.5 % and rose to ~ 2.5 % for the λ = 0.250 case.

Removal of N_2 from the exhaust stream before recirculation to the gasifier actually has a slightly negative effect on system performance compared to the original simulation for low to moderate amounts of exhaust recycling. This highlights the importance of the exhaust gases in reusing waste heat. Since the N_2 species is inert in the gasifier, we can

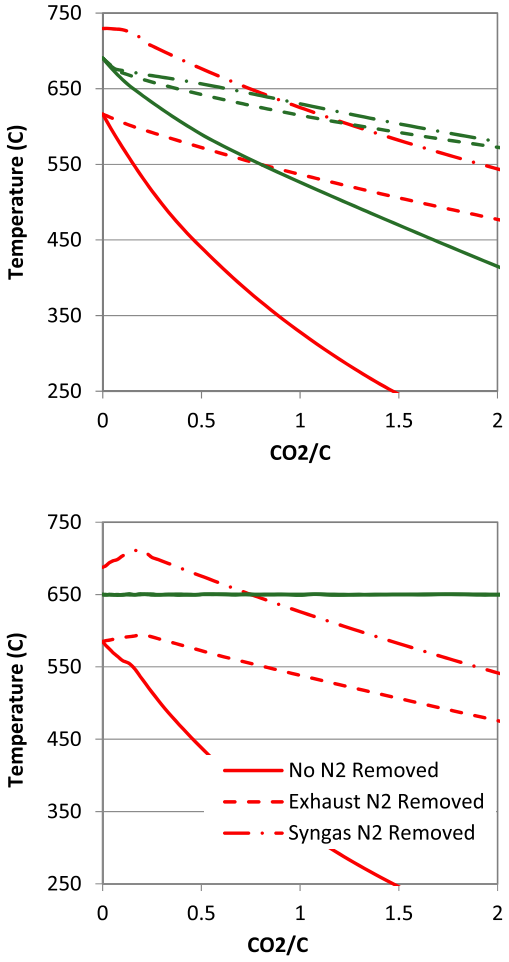

Fig. 10. Effect of nitrogen removal on EGT in red and gasifier temperature in green for λ = 0.250 (top) and constant temperature 650 °C (bottom).

see here the effect of supplying additional heat to the gasifier through the mass flow of exhaust N_2 compared to the case where it is removed from the exhaust. It appears that the lower temperature of the N_2 diluted exhaust is offset by the increased mass flow of the exhaust stream to the gasifier, thus carrying more thermal energy into the gasifier. This result is eventually negated at higher recycling ratios as the continuous build-up of N_2 diluent causes a rapid decrease in EGT as the recycling ratio accumulates.

Precombustion diluent removal also improves the performance when constant temperature gasification is used. Fig. 11 demonstrates this effect is most pronounced for lower gasifier temperatures since the higher EGTs will have a greater allothermal heating effect, particularly for the 650 °C and 700 °C gasifier temperature cases at low recycling ratios when EGTs are above the gasifier equilibrium temperature. Again, the removal of diluent from the exhaust stream in the second case has a marginally negative impact on overall system performance for the same reasons highlighted above. Peak system efficiencies of 31.17 % and 30.84 % were reported at recycling ratios of 0.220 and 0.163 mol CO_2/mol C for pre-combustion N_2 removal at the constant gasifier temperatures of 650 °C and 700 °C, respectively.

4.3. *Assessment of CO_2 utilisation and emissions*

Analysis has so far focused on the overall system performance and thermal integration of the gasifier and engine exhaust. Assessment of the CO_2 utilisation within the system will also provide insight on the most effective CDU aspects of EGR enhanced gasification. To determine the

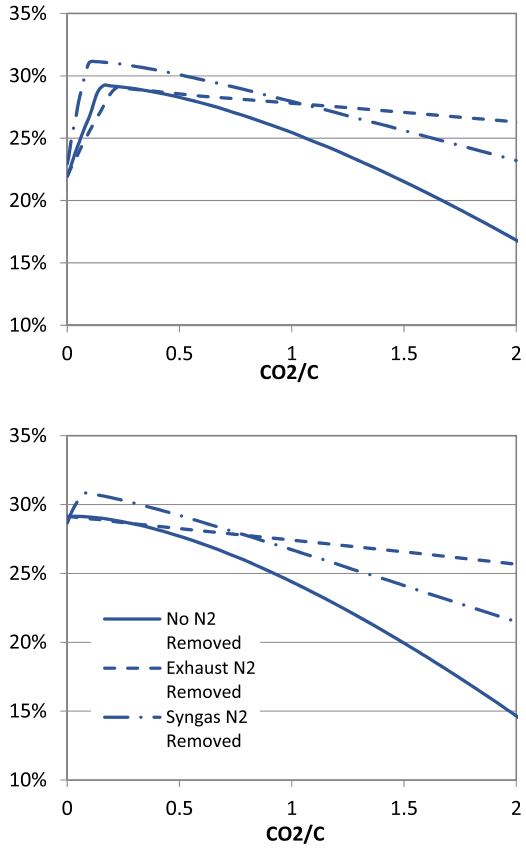

Fig. 11. System efficiency for constant gasifier temperatures of 650 °C (top) and 700 °C (bottom).

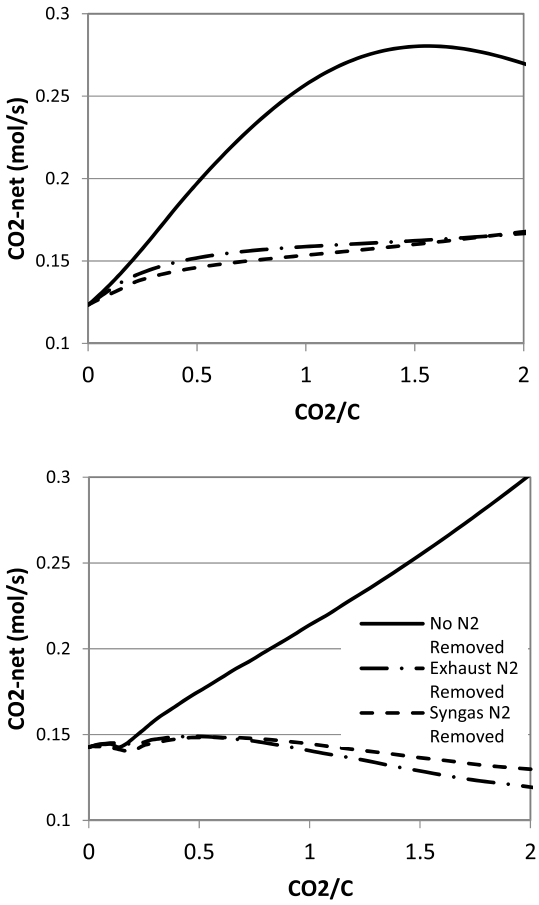

Fig. 12. Net CO_2 production in the gasifier for (top) constant $\lambda = 0.25$ and (bottom) constant gasifier temperature of 650 °C.

actual generation rate of CO_2 from gasification, the gasifier's net CO_2 production is calculated as the difference between the CO_2 content in the syngas and the amount of CO_2 supplied to the gasifier as a gasifying agent (Equation (17)). In this way the CO_2 generated during gasification is distinguished from the CO_2 recycled to the gasifier from the engine exhaust.

$$CO_{2,net} = CO_{2,syngas} - CO_{2,EGR} \quad (17)$$

Fig. 12 shows a trend that, in general, net CO_2 increases with recycling ratio, indicating that recycled CO_2 is not being consumed in the gasifier. This is due to the lower gasifier temperatures (see Fig. 6) which will not favour the endothermic reactions that convert CO_2 to syngas. As examples of this situation, the equilibrium constants (see Table 4) of the reverse Boudouard (equation (1)), reverse WGS (equation (2)), and methane dry-reforming (equation(3)) reactions demonstrate a marked downward shift for temperatures corresponding to increased recycling ratios, often in orders of magnitude. Such changes mean the reactants (including CO_2) become thermodynamically favoured over the products of those reactions. Mathematically, this behaviour is predictable from the calculation of the equilibrium constant from fundamental thermodynamic principles as $K_p = \exp(-\Delta G/RT)$. This effect is further evidenced by the corresponding reductions in CO production discussed previously in Fig. 5 and Fig. 7 due to these same temperature-induced equilibrium shifts in the WGS and dry-reforming reactions that favour CO_2 over CO. Higher recycling ratios at constant air ratios indicate an eventual benefit of concentration-based shifts to the CO_2 equilibrium in the gasifier, however the corresponding syngas is very dilute, carbon conversion is poor, and the equilibrium temperature is so low that gasification may not be achievable in practise.

For the 650 °C constant gasifier temperature case, the continuous increase in air ratio required to maintain the gasification temperature will favour the oxidation reactions, thus increasing the net production of CO_2 in a nearly linear fashion beyond the carbon boundary. Although reaction equilibrium constants will remain the same at the constant gasification temperature, the increase in O_2 supply to the gasifier promotes the formation of CO_2 through combustion reactions. While partial char oxidation reactions would generate some CO due to the increase in O_2 supply up to the carbon boundary, CO_2 remains the thermodynamically favoured product given the significant difference in equilibrium constants since $K_{p,comb} \gg K_{p,p\text{-}ox}$. Additionally, CO combustion reactions will contribute to a decrease in CO and a corresponding increase in CO_2 as additional O_2 is supplied beyond the carbon boundary.

A minor improvement in CO_2 conversion occurs for low amounts of exhaust recycling in the constant temperature gasifier. However, net CO_2 production only decreased by approximately 1.00 % from initial conditions up to the point of full char conversion while O_2 input increases by 44.04 % further indicating the gasification thermodynamic conditions favour char oxidation reactions over the reverse Boudouard reaction. Despite the limited CO_2 conversion for the constant temperature case up to the carbon boundary, it otherwise appears that the

Table 4
Equilibrium constants for reverse Boudouard (1), reverse water-gas shift (2), and methane dry-reforming (3) reactions under exhaust recycling ratios at corresponding gasifier temperatures.

CO_2/C	Temp (°C)	$K_{p,1}$	$K_{p,2}$	$K_{p,3}$
0	690.5	$8.50*10^{-1}$	$6.33*10^{-1}$	$5.19*10^{0}$
0.508	524.7	$1.01*10^{-2}$	$2.56*10^{-1}$	$5.88*10^{-3}$
1.034	408.4	$1.22*10^{-3}$	$1.01*10^{-1}$	$7.25*10^{-6}$

recycled CO_2 is not active in any chemical reactions to produce fuel since the net CO_2 production from the gasifier continues to increase. In this instance the increase in system performance is attributable to CO_2 and other exhaust gases acting primarily as a heat transfer medium to recycle heat rejected from the engine cycle to the gasifier.

N_2 dilution in the system has a significant, negative impact on these CO_2 utilisation trends. For the cases where N_2 is removed from the syngas or exhaust gases, dramatic reductions in gasifier CO_2 generation are evident over the same recycling ratios. In the first instance, removal of excess N_2 effectively increases the concentration of CO_2 in the gasifier as exhaust gases are recycled, even though the total amount of CO_2 supplied to the gasifier is the same as before. This is in contrast to the original cases where N_2 concentrations in the syngas were typically above 40 % by volume and tended to approach 80 % at very high recycling ratios. Additionally, the increases in EGT when N_2 is removed allowed for higher gasifier temperatures, making favourable conditions for endothermic reactions to consume CO_2. In fact, a 1.74 % improvement in CO_2 conversion occurs at the carbon boundary for the 650 °C constant temperature gasifier before a moderate increase in net CO_2 production. This operating point is near the peak EGT condition. Additionally, the higher temperature recycled exhaust heat minimised the required air flow to maintain the constant gasifier temperature, allowing for net CO_2 production to once again decrease at higher recycling ratios. This is consistent with experimental results that indicate best CO_2 conversion conditions exists at the highest temperatures [9].

Although the chemical utilisation of CO_2 as a gasifying reagent tends to be poor, the modest improvements to indicated power and system efficiency from exhaust recycling will affect specific emissions released from the power cycle. Under all system configurations, the local minima of indicated specific CO_2 emissions occur at the best efficiency points, highlighting the importance of gasifier equilibrium conditions on the overall system performance. In the context of biomass energy, this aspect becomes important due to the delay between CO_2 emissions from the power cycle and the reabsorption of the carbon into the next generation of feedstock required to make the cycle carbon neutral. While there is considerable variability in the extent of this “carbon debt” [37,38] it stands to reason that any improvement in bioenergy specific emissions will be beneficial in reducing the carbon debt for a given rate of bioenergy generation.

While it seems there are marginal benefits in the gasifier’s CO_2 consumption at higher recycling ratios, the dilute, low-quality syngas produced under these conditions drastically reduces both the CGE and the engine’s indicated power output. Regardless of the gasifier’s CO_2 conversion conditions, use of EGR enhanced gasification successfully reduced the indicated specific CO_2 emissions at the optimal efficiency operation points. Table 5 summarises the system efficiencies and CO_2 emissions for these key cases, underscoring the combined effect of air ratio and recycling ratio on the overall system performance. Although the increase to system efficiency is minor, EGR gasification at an air ratio of $\lambda = 0.250$ would reduce the specific CO_2 emissions by 46.2 g/kWh, a 3.79 % decrease from the original system configuration at $\lambda = 0.300$.

Table 5
Summary of combined system efficiency and specific CO_2 emissions for select system configurations.

Air Ratio, λ	Gasification Temperature	N_2 Removal	Recycling Ratio	Combined System Efficiency	Specific CO_2 Emissions (g-CO_2/kWh)
0.300	(972 °C)	–	–	28.14 %	1218.5
0.300	(788 °C)	–	0.219	28.21 %	1215.4
0.250	(654 °C)	–	0.136	29.24 %	1172.3
(0.251)	650 °C	–	0.163	29.23 %	1172.4
(0.260)	700 °C	–	0.020	29.15 %	1176.1
0.250	(669 °C)	from Syngas	0.220	31.02 %	1104.3
(0.241)	650 °C	from Syngas	0.220	31.17 %	1100.0
(0.260)	700 °C	from Syngas	0.163	30.84 %	1111.6

*Dependent gasification variable indicated in parentheses.

Significant emissions improvement would be achieved if inert diluents could be removed from the syngas or if gasification temperatures could be increased. In addition to the efficiency benefits previously discussed, pre-combustion N_2 removal would decrease indicated CO_2 emissions by 9.73 %, emitting 118.5 g/kWh less than the basic system.

5. Conclusions

Analysis of a representative numerical model has quantified the capacity for direct CDU in a small-scale, air-blown, biomass gasification power cycle using EGR enhanced gasification. Key conclusions relating to thermodynamic gasification conditions and system responses are as follows:

- Marginal improvements in indicated output power, system efficiency, and specific emissions are observed under modest exhaust recycling conditions.
- Over certain ranges, EGR supply to the gasifier can lower the air ratio required in the gasifier to maintain full carbon conversion, thus increasing CGE.
- Recycling 0.136 mol-CO_2/mol-C to a gasifier with an air-ratio of $\lambda = 0.250$ increased overall system efficiency by 1.1 % and reduced the specific CO_2 emissions by 46.2 g-CO_2/kWh compared to the reference system configuration.
- Exhaust recycling dilutes the syngas with excess N_2 and CO_2, resulting in a lower LHV, lower EGT, and thus lower equilibrium temperatures. High amounts of EGR limits gasifier thermodynamic performance since lower equilibrium temperatures cause lower CO_2 conversion and thus lower syngas quality.
- Gasification equilibrium temperatures dropped by 318 °C from the reference case when the gasifier had 0.136 mol-CO_2/mol-C of exhaust recycled and the air-ratio reduced to $\lambda = 0.250$. The net-CO_2 utilisation decreases and the H_2:CO ratio tends to increase with exhaust recycling due to lower equilibrium temperatures.
- Modelling techniques revealed the impact of N_2 dilution is most prevalent in the engine exhaust temperatures. In total, syngas N_2 dilution lowers the overall system efficiency by 2.5 percentage points and increases specific emissions by 72.4 g-kWh, or 6.16 %, compared to a N_2-free syngas. This suggests CDU aspects of the system could be further enhanced if additional syngas upgrading or diluent removal is implemented.
- Due to unfavourable thermodynamic conditions in the gasifier, most cases studied showed poor CO_2 conversion to syngas. This indicates the primary use of recycled CO_2 under these conditions is as a heat transfer medium rather than chemically active reagent. Evidence of enhanced CO_2 chemical conversion to CO is limited to the point of full char conversion in 650 °C gasifiers, with N_2 dilution of the syngas also diminishing this effect.

This technical assessment has highlighted the thermodynamic benefits and limitations of EGR enhanced gasification as a direct CDU strategy for a biomass IGC, leading to a detailed understanding of the system thermodynamic conditions under different operating points. It provides a system-level understanding of how EGR influences an IGC and serves as a baseline for future detailed analysis including specific gasifier designs. Given the modest improvements to system performance, following work should also adopt an economic scope to determine the feasibility and potential impact of this CDU strategy when applied in practise.

CRediT authorship contribution statement

Michael J. Greencorn: Conceptualization, Methodology, Software, Validation, Investigation, Formal analysis, Visualization, Writing – original draft, Writing – review & editing. **S. David Jackson:** Supervision, Writing – review & editing. **Justin S.J. Hargreaves:** Supervision, Writing – review & editing. **Souvik Datta:** Supervision, Writing – review & editing. **Manosh C. Paul:** Conceptualization, Supervision, Writing – review & editing, Project administration, Funding acquisition.

Declaration of Competing Interest

The authors declare that they have no known competing financial interests or personal relationships that could have appeared to influence the work reported in this paper.

Acknowledgment

This research was supported by the University of Glasgow's Lord Kelvin/Adam Smith (LKAS) PhD Scholarship.

References

[1] IEA, "About CCUS," International Energy Agency, Paris; 2021.
[2] IEA, "Bioenergy Power Generation," International Energy Agency, Paris; 2020.
[3] IPCC, "IPCC special report on the impacts of global warming of 1.5 °C above pre-industrial levels and related global greenhouse gas emission pathways," V. Masson-Delmotte, P. Zhai, H. O. Portner, D. Roberts, J. Skea, P. R. Shukla, A. Pirani, W. Moufouma-Okia, C. Pean, R. Pidcock, S. Connors, J. B. R. Matthews, Y. Chen, X. Zhou, M. I. Gomis, E. Lonnoy, Maycock, M. Tignor and T. Waterfield, Eds., Geneva, Switzerland, World Meteorological Organization; 2018.
[4] Basu P. Biomass gasification and pyrolysis: Practical design and theory, 2nd ed., Boston: Academic Press; 2013.
[5] Ahmed I, Gupta AK. Characteristics of cardboard and paper gasification with CO2. Appl Energy 2009;86:2626–34.
[6] Guizani C, Louisnard O, Escudero Sanz FJ, Salvador S. Gasification of woody biomass under high heating rate conditions in pure CO2: Experiments and modelling. Biomass Bioenergy 2015;83:169–82.
[7] Ahmed II, Gupta AK. Kinetics of woodchips char gasification with steam and carbon dioxide. Appl Energy 2011;88:1613–9.
[8] Prabowo B, Umeki K, Yan M, Nakamura MR, Castaldi MJ, Yoshikawa K. CO2–steam mixture for direct and indirect gasification of rice straw in a downdraft gasifier: Laboratory-scale experiments and performance prediction. Appl Energy 2014;113:670–9.
[9] Janganathan VM, Varunkumar S. Net carbon-dioxide conversion and other novel features of packed bed biomass gasification with O2/CO2 mixtures. Fuel 2019;244:545–58.
[10] Prabowo B, Susanto H, Umeki K, Yan M, Yoshikawa K. Pilot scale autothermal gasification of coconut shell with CO2-O2 mixture. Front. Energy 2015;9(3):362–70.
[11] Ravikiran A, Renganathan T, Pushpavanam S, Voolapalli RK, Cho YS. Generalized Analysis of Gasifier Performance using Equilibrium Modeling. Ind Eng Chem Res 2012;51:1601–11.
[12] Renganathan T, Yadav MV, Pushpavanam S, Voolapalli RK, Cho YS. CO2 utilization for gasification of carbonaceous feedstocks: A thermodynamic analysis. Chem Eng Sci 2012;83:159–70.
[13] Chaiwatanodom P, Vivanpatarakij S, Assabumrungrat S. Thermodynamic analysis of biomass gasification with CO2 recycle for synthesis gas production. Appl Energy 2014;114:10–7.
[14] Wang L, Izaharuddin AN, Karimi N, Paul MC. A numerical investigation of CO2 gasification of biomass particles-analysis of energy, exergy and entropy generation. Energy 2021;228:120615.
[15] Hepburn C, Adlen E, Beddington J, Carter EA, Fuss S, MacDowell N, et al. The technological and economic prospects for CO2 utilization and removal. Nature 2019;575:87–97.
[16] Walker ME, Abbasian J, Chmielewski DJ, Castaldi MJ. Dry Gasification Oxy-combustion Power Cycle. Energy Fuels 2011;25:2258–66.
[17] Ishii H, Hayashi T, Tada H, Yokohama K, Takashima R, Hayashi J-I. Critical assessment of oxy-fuel integrated coal gasification combined cycles. Appl Energy 2019:156–69.
[18] Oki Y, Hamada H, Kobayashi M, Yuri I, Hara S. Development of high-efficiency oxy-fuel IGCC system. In: Energy Procedia, Lausanne, Switzerland; 2017.
[19] Prabowo B, Aziz M, Umeki K, Susanto H, Yan M, Yoshikawa K. CO2-recycling biomass gasification system for highly efficient and carbon-negative power generation. Appl Energy 2015;158:97–106.
[20] Indrawan N, Kumar A, Moliere M, Sallam KA, Huhnke RL. Distributed power generation via gasification of biomass and municipal solid waste: A review. J Energy Inst 2020;93:2293–313.
[21] Breeze PA. Combined Heat and Power, London: Elsevier; 2018.
[22] Perez NP, Machin EB, Pedroso DT, Roberts JJ, Antunes JS, Silveira JL. Biomass gasification for combined heat and power generation in the Cuban context: Energetic and economic analysis. Appl Therm Eng 2015;90:1–12.
[23] Milne TA, Evans RJ, Abatzoglou N. Biomass Gasifier Tars: Their Nature, Formation, and Conversion. National Renewable Energy Laboratory, Golden, Colorado; 1998.
[24] Salem AM, Zaini IN, Paul MC, Yang W. The evolution and formation of tar species in a downdraft gasifier: Numerical modelling and experimental validation. Biomass Bioenergy 2019;130:105377.
[25] Mazzola S, Astolfi M, Macchi E. The potential role of solid biomass for rural electrification: A techno economic analysis for a hybrid microgrid in India. Appl Energy 2016;169:370–83.
[26] Ren H, Gao W. A MILP model for integrated plan and evaluation of distributed energy systems. Appl Energy 2010;87(3):1001–14.
[27] Greencorn MJ, Jackson SD, Hargreaves JSJ, Datta S, Paul MC. A novel BECCS power cycle using CO2 exhaust gas recycling to enhance biomass gasification. In: International Conference on Applied Energy 2019, Västerås, Sweden; 2019.
[28] Simone M, Barontini F, Nicolella C, Tognotti L. Gasification of pelletized biomass in a pilot scale downdraft gasifier. Bioresour Technol 2012;116:403–12.
[29] Ji-chao Y, Sobhani B. Integration of biomass gasification with a supercritical CO2 and Kalina cycles in a combined heating and power system: A thermodynamic and exergoeconomic analysis. Energy 2021;222:119980.
[30] Hamrang F, Shokri A, Mahmoudi SMS, Ehghaghi B, Rosen M. Performance Analysis of a New Electricity and Freshwater Production System Based on an Integrated Gasification Combined Cycle and Multi-Effect Desalination. Sustainability 2020;12(19):7996.
[31] Heywood JB. Internal Combustion Engine Fundamentals, New York: McGraw-Hill; 1988.
[32] Ferguson CR, Kirkpatrick T. Internal Combustion Engines Applied Thermosciences, 3rd ed., Chichester: John Wiley & Sons; 2016.
[33] Shivapuji AM, Dasappa S. Analysis of thermodynamic scope engine simulation model empirical coefficients: Suitability assessment and tuning of conventional hydrocarbon fuel coefficients for bio syngas. Int J Hydrogen Energy, 2017;42(26):16834-16854 [29 6 2017].
[34] Annand WJD. Heat Transfer in the Cylinders of Reciprocating Internal Combustion Engines. Proc Inst Mech Eng 1963;177(36):973–96.
[35] Shivapuji AM, Dasappa S. Experiments and Zero D Modeling Studies Using Specific Weibe Coefficients for Producer Gas as Fuel in Spark-ignited Engines. Proc Inst Mech Eng, Part C: J Mech Eng Sci 2012;227(3):504–19.
[36] Greencorn MJ, Jackson SD, Hargreaves JSJ, Datta S, Paul MC. Modelling the performance of a syngas fueled engine: Effect of excess air and CO2 as combustion diluents. In: Low-Carbon Combustion Joint Meeting of the French and British Sections of the Combustion Institute, Lille, France; 2020.
[37] Liu W, Peng C, Chen Z, Liu Y, Yan J, Li J, et al. Sustainable bioenergy production with little carbon debt in the Loess Plateau of China. Biotechnol Biofuels 2016;9(161).
[38] Bentsen NS. Carbon debt and payback time – Lost in the forest? Renew Sustain Energy Rev 2017;73:1211–7.